IEEE NPSS (Toronto), UOIT, Oshawa, ON, 25 & 26 June, 2010
International Workshop on Real Time Measurement, Instrumentation & Control [RTMIC]

# Tissue Segmentation in Medical Images Based on Image Processing Chain Optimization

S. Rahnamayan, Z. S. Mohamad
Faculty of Engineering and Applied Science
University of Ontario Institute of Technology (UOIT), Oshawa, Canada
Shahryar.Rahnamayan@uoit.ca, zaid.mohamad@uoit.ca

**Abstract**

Segmentation is a crucial task in medical image processing. The accuracy of the segmentation can directly affect other post processing tasks, such as image analysis and feature extraction. Knowledge and sample based learning approaches play a pivotal role in an image processing. However, the acquisition and integration of expert knowledge (for the former) and providing a sufficiently large number of training samples (for the latter) are generally hard to perform and time consuming tasks. Hence, learning image processing tasks from a few gold/ground truth samples (three for the current work), prepared by the radiologist, is highly desirable. The purposed approach utilizes Differential Evolution (DE) to optimize an image processing chain; which has successfully been used to segment breast ultrasound and X-ray lung images. The training is based on three sample images provided by an expert. As a case study, for each image modalities (ultrasound and x-ray), six test images are used for performance investigation. Details about the proposed algorithm and also conducted experiments are provided.

**Keywords:** Lung segmentation, Breast segmentation, Differential Evolution (DE), Ultrasound, X-ray, Medical image processing

## 1. Introduction

Breast ultrasound and x-ray lung segmentations has a great role in detection of cancer disease; early detection can be helpful for effective treatment. Segmentation has become one of the main tasks for medical image processing. Many algorithms were developed to increase the accuracy of the segmented image such as Snakes or Active Contour Models (ACM). Numerous image segmentation techniques have already been proposed. Shi et. al. introduced SIFT local descriptor Scale In-variant Feature Transform to characterize the image feature in the vicinity of each pixel [4]. They also used a deformable model which is constrained by both population-based and patient-specific shape statistics. Xu et. al. proposed a modified gradient vector flow based active shape model (GVF-ASM) for lung field extraction from chest radiographs. This Technique provided around 3-5% improvement over the ASM techniques. However, majority of the available methods are application- or domain- oriented solutions suffering from lack of universality. Therefore, this research filed is still open to investigate and introduce new robust and universal techniques. The current work is mainly based on the previous work, which was about the automatic acquisition of image filtering and object extraction procedures from ground-truth samples [2]. Similarly, the proposed approach in this paper is based on learning from a few ground-truth images segmented manually by a radiologist. It accepts three sample images and their corresponding segmented (ground-truth) images for the offline optimization of an image processing chain. During this phase, Differential Evolution (DE), as an effective optimization algorithm, optimizes the chain of image processing tasks by selecting desirable algorithms and corresponding optimal parameters for each algorithm. The image processing chain contains image filtering, contrast enhancement, thresholding, and post-processing tasks. After terminating the one-time training (optimization) phase, the achieved optimal chain is ready to process other images from the same modality to extract the specific tissue of the image. The approach can be mentioned as a semi-automated method, because user just needs to enter one seed point by clicking on the tissue (region of the interest). The approach is not limited to ultrasound or x-ray image segmentation; although, these two modalities are used as case studies in the current work. It can be applied to segment other sort of medical (e.g., lung CT images) or even non-medical (e.g., industrial) images successfully. All details about the proposed algorithm and experimental verifications are provided.

The organization of the paper is as follows: Section 2 presents a short review of the Differential Evolution (DE) algorithm which has been utilized to optimize the image processing chain. Section 3 explains the proposed approach briefly. Experimental verifications are given in Section 4 and finally the paper is concluded in Section 5.

## 2. Differential Evolution: A Short Review

Differential Evolution (DE) grew out of Ken Price's attempts to solve the Chebychev Polynomial fitting Problem that had been posed to him by Rainer Storn [1]. A breakthrough happened, when Ken came up with the idea of using vector differences for perturbing the vector population. DE calculates numerical optimization without explicit knowledge of the gradient of the problem to be optimized and works on multi-dimensional real-valued functions which are not necessarily continuous or differentiable.

DE is a simple effective and robust population-based optimization algorithm. The main idea behind DE is a scheme for generating trial parameter vectors. Basically, for every vector in the population (called target vector), DE selects randomly two other vectors, subtract them and adds the weighted difference to a randomly chosen third vector (called the base vector) to produce a mutant vector. Then for every vector in the mutant population, we use a user-defined value called Crossover rate (Cr) to control the fraction of parameter values that are copied from the mutant and Target vector to the trial vector. Finally, for the selection step, if the trial vector has an equal or lower fitness value (for minimization problem) than that of its target vector, it replaces the target vector in the next generation; otherwise, the target retains its place in the population for at least one more generation. This steps are repeated for every vector in the population to produce the next new population. Algorithm 1 presents pseudocode of the classical Differential Evolution (DE) algorithm [1]. Three main operators (mutation, crossover, and selection) are given in lines 5-6, 7-13, and 15-19, respectively.

**Algorithm 1** Differential Evolution (DE). $P_0$: Initial population, $N_p$: Population size, $V$: Noise vector, $U$: Trial vector, $D$: Problem dimension, BFV: Best fitness value so far, VTR: Value-to-reach, NFC: Number of function calls, $\text{MAX}_{\text{NFC}}$: Maximum number of function calls, F: Mutation constant, $rand(0,1)$: Uniformly generated random number, $C_r$: Crossover rate, $f(\cdot)$: Objective function, $P'$: Population of the next generation.

Generate uniformly distributed random population $P_0$
**while** ( BFV $>$ VTR **and** NFC $< \text{MAX}_{\text{NFC}}$ ) **do**
  //Generate-and-Test-Loop
  **for** $i = 0$ to $N_p$ **do**
    Select three parents $X_a$, $X_b$, and $X_c$ randomly from current population where $i \neq a \neq b \neq c$
    //Mutation
    $V_i \leftarrow X_a + F \times (X_c - X_b)$
    //Crossover
    **for** $j = 0$ to $D$ **do**
      **if** $rand(0,1) < C_r$ **then**
        $U_{i,j} \leftarrow V_{i,j}$
      **else**
        $U_{i,j} \leftarrow X_{i,j}$
      **end if**
    **end for**
    //Selection
    Evaluate $U_i$
    **if** $(f(U_i) \leq f(X_i))$ **then**
      $X'_i \leftarrow U_i$
    **else**
      $X'_i \leftarrow X_i$
    **end if**
  **end for**
  $X \leftarrow X'$
**end while**

## 3. Proposed Approach

The proposed image processing chain for tissue segmentation includes pre-processing, thresholding, and post-processing tasks. The pre-processing contains image filtering and contrast enhancement. Post-processing is equipped with mathematical morphology operations such as dilation, erosion, opening, and closing. Each image processing algorithm has own parameters which should be tuned for optimality. In order to find the optimal combination of the algorithms for each step and also optimal parameter tuning for each selected algorithm, an effective evolutionary algorithm (DE) has been employed, Figure 1.

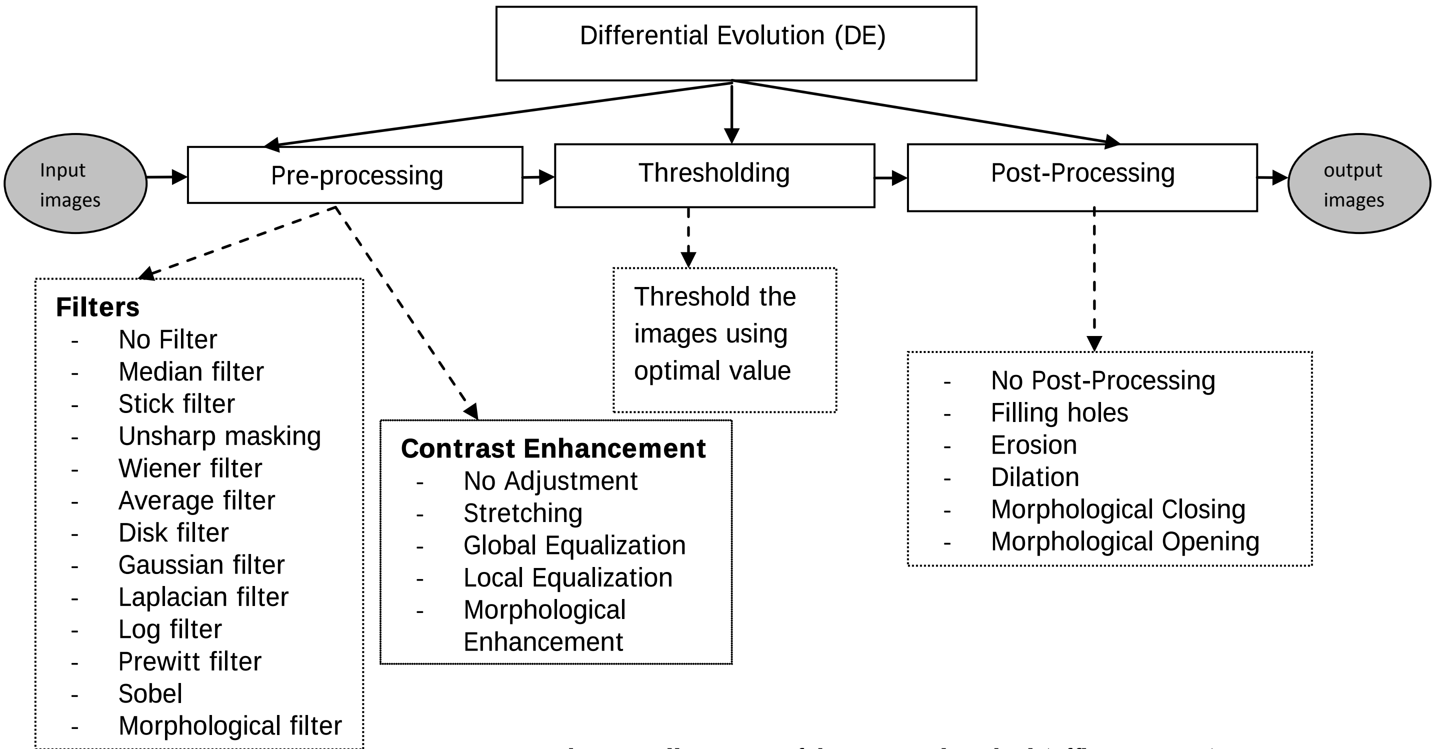


Figure 1: Schematic illustration of the proposed method (offline training).

Three sample images and their corresponding ground-truth images are the inputs for the proposed method, the optimizer (DE) tries to maximize overlapping among the resulted images and the ground-truth images. By this way, it tries to find the optimal image processing chain to extract a specific tissue from a medical image modality. After terminating the optimization phase, the chain would be ready to accept new images to extract the tissue just by getting one seed point inside the tissue via a mouse clicking.

## 4 Experimental Verifications

In order to investigate performance of the proposed approach, it is applied to segmentation of x-ray lung and ultrasound breast images. The numerical results and visualizations are provided in the following two sections. For each case, the image processing chain is optimized by using three sample images and then the obtained optimal chain has been utilized to segment six new test images for each imaging modality.

Following definitions and metrics (i.e., precision, sensitivity, and overlapping ratios) are utilized to report the numerical results of our experiments.

- True positive: Tissue pixcel (foreground) is correctly diagnosed as tissue pixcel
- False positive: Non-tissue pixcel (background) incorrectly identified as tissue pixcel
- True negative: Non-tissue pixcel correctly identified as Non-tissue pixcel
- False negative: Tissue pixcel incorrectly identified as Non-tissue pixcel

***Precision*** = *(number of true negative pixels)/( number of true negative pixels + number of false positive pixels)  (1)*
***Sensitivity*** = *(number of true positive pixels)/( number of true positive pixels + number of false negetive pixels)  (2)*
***Overlap*** = *(number of true positive pixels + number of true negative pixels)/number of total pixels  (3)*

## 4.1 X-ray Lung Segmentation

Figure 2 presents three input grey-level x-ray lung images, the corresponding gold images, and the resulted output images of the chain optimization phase. The gold images are provided by an expert. It has been tried to select images with different contrast level and tissue shape for the training set.

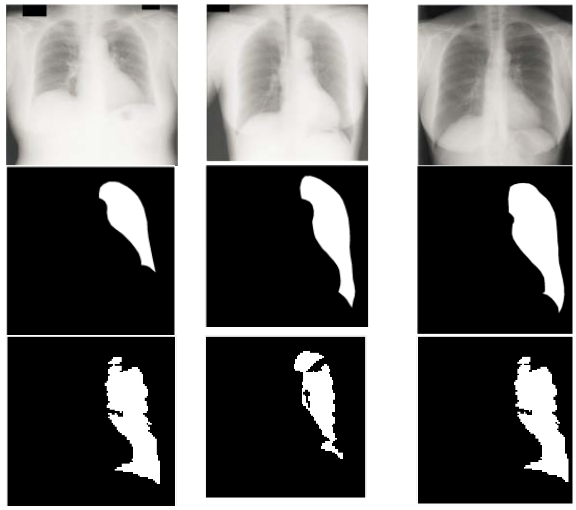

Figure 2: Three training X-ray lung images (the first row) with their corresponding gold/ground-truth images (the second row) and the chain optimization results (the third row).

Now, the optimal image processing chain is obtained and that is ready to be applied to the new images. Figure 3 illustrates six x-ray lung images and corresponding tissue segmentation results. The green segmentation shows ground-truth segmentation (performed by a radiologist) and the red one presents the result of the proposed approach. As seen, the ground-truth segmentation is smoother; because it doesn't follow the exact border of the edges and knowledge of the radiologist has been employed instead of pixels' grey-level.

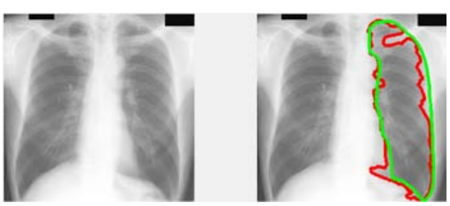

Image 1

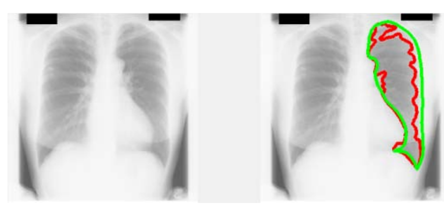

Image 2

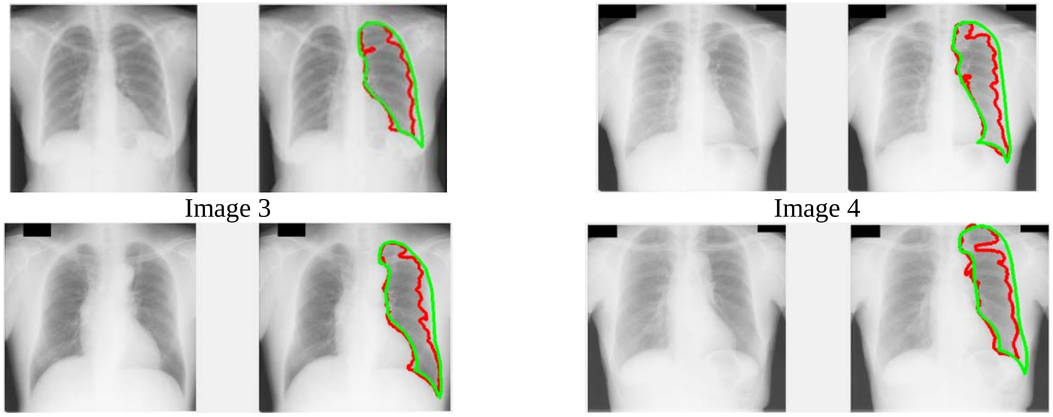


Figure 3: Six test X-ray lung images and corresponding tissue extraction results. The green segmentation (light-grey in a grey-level printing) has been performed by a radiologist and the red (dark-grey in a grey-level printing) one by the proposed method.

Numerical results for the mentioned six images are provided in Table 1. As shown, the average of sensitivity, precision rate, and the overlap ratio are 78.3%, 94.2%, and 74.8%, respectively; which is promising.

| *Image* | *Sensitivity (%)* | *Precision Rate (%)* | *Overlap Ratio (%)* |
|---|---|---|---|
| Image 1 | 87 | 92 | 81 |
| Image 2 | 73 | 96 | 71 |
| Image 3 | 82 | 96 | 80 |
| Image 4 | 75 | 96 | 73 |
| Image 5 | 78 | 93 | 74 |
| Image 6 | 75 | 92 | 70 |
| **Ave.** | **78.3** | **94.2** | **74.8** |

Table 1: Numerical results for six X-ray Lung images. The sensitivity, precision rate, and the overlap ratio are reported for each test image.

## 4.2 Ultrasound Breast Cancer/Cyst Extraction

Similar to Lung segmentation, we have used three images with corresponding gold images to optimize the proposed chain for segmentation of ultrasound breast cancer/cyst images, Figure 4.

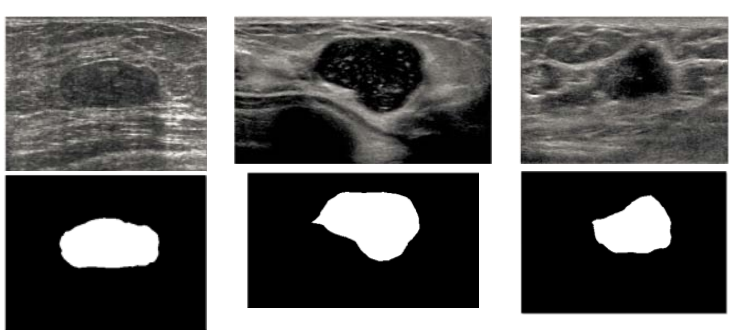

Figure 4: Three training ultrasound breast images (the first row) with their corresponding gold/ground-truth images (the second row) and the offline training results (the third row).

The obtained optimal image processing chain has been applied to the new test images. Figure 5 illustrates six ultrasound breast images and the corresponding tissue segmentation results. Similarly, the green segmentation has been performed by a radiologist and the red one by the proposed method.

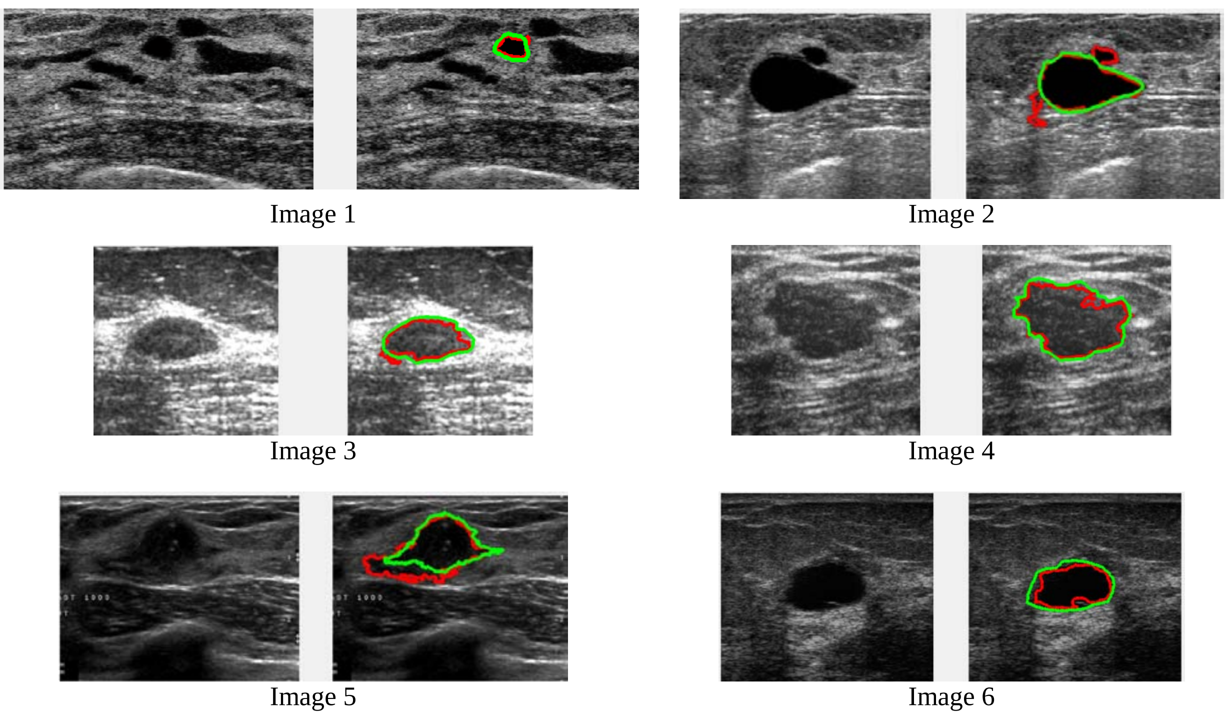


Figure 5: Six test ultrasound breast images and corresponding tissue extraction results. The green segmentation (light-grey in a grey-level printing) has been performed by a radiologist and the red (dark-grey in a grey-level printing) one by the proposed method.

Numerical results for the mentioned six images are provided in Table 2. As shown, the average of sensitivity, precision rate, and the overlap ratio are 81.8%, 91.8%, and 75.3%, respectively. Similar to the previous case the average overlapping is about 75%. The difference between the similar metrics for the two experimental series (lung and breast) is less than 4%. It confirms that, the image processing chain has been optimized for each image modality properly.

| *Image* | *Sensitivity (%)* | *Precision Rate (%)* | *Overlap Ratio (%)* |
|---|---|---|---|
| Image 1 | 76 | 96 | 74 |
| Image 2 | 92 | 86 | 80 |
| Image 3 | 77 | 97 | 75 |
| Image 4 | 84 | 100 | 84 |
| Image 5 | 90 | 72 | 67 |
| Image 6 | 72 | 100 | 72 |
| **Ave.** | **81.8** | **91.8** | **75.3** |

Table 2: Numerical results for six ultrasound breast images. The sensitivity, precision rate, and the overlap ratio are reported for each test image.

## 5. Conclusion Remarks

In this paper, a novel medical image segmentation algorithm has been proposed and tested successfully with ultrasound breast images and x-ray lung images. However, that is not limited to the mentioned medical image modalities and even can be applied to non-medical images, by this way, it supports a remarkable level of the universality. Unlike to other similar methods, thie method is not a problem-oriented solution for the image segmentation. The experimental results are presented by visualization and comparison with the provided gold images by using three well-known measures, namely, sensitivity, precision rate, and overlapping ratio. Obtained numerical results are promising. As a future work, we will enrich the image processing chain by using more algorithms in both pre- and post-processing phases; furthermore, other optimization method will be investigated to solve the combinatorial part of the chain optimization problem.

## References

[1]. K.V. Price, R.M. Storn, J.A. Lampinen, *Differential Evolution A Practical Approach to Global Optimization,* Springer, 2005, ISBN:3540209506.

[2]. S. Rahnamayan, H.R. Tizhoosh, M.M.A. Salama, *Automatic Acquisition of Image Filtering and Object Extraction Procedures from Ground-Truth Samples*, Journal of Advanced Computational Intelligence and Intelligent Informatics, Volume 13, No. 2, March 2009, pp. 115-127.

[3]. C. Wang, S. Guo, X. Wu, Segmentation of Lung region for chest X-ray images based on medical registration and ASM, International Conference on Bioinformatics and Biomedical Engineering , Beijing, China, June 2009 pp. 1-4.

[4]. Y. Shi, F. Qi, Z. Xue, . Chen, K. Ito, H. Matsuo, D. Shen, *Segmenting Lung Fields in Serial Chest Radiographs Using Both Population-Based And Patient-Specific Shape statistics*, IEEE Transactions on Medical Imaging, Vol.. 27, No. 4, April 2008, pp. 481 - 494.

[5]. T. Xu, M. Mandal, R. Long and A. Basu, *Gradient Vector Flow based Active Shape Model for Lung Field Segmentation in Chest Radiographs*, 31st Annual International Conference of the IEEE Eng. Med. Bio. Soc., Minneapolis, Minnesota, USA, Sep. 2-6, 2009, pp. 3561-3564.

## Authors' Short Biography

**Dr. Shahryar Rahnamayan** received his B.Sc. and M.Sc. degrees in software engineering. In 2007, he received his Ph.D. degree in the field of evolutionary computation from University of Waterloo (UW), Canada. The opposition-based differential evolution (ODE) was proposed in his PhD thesis. Since August 2007, he has been a chief research manager at OMISA Inc. (Omni-Modality Intelligent Segmentation Assistant); a company which develops innovative software for medical image segmentation. Before joining to faculty of engineering and applied science, University of Ontario Institute of Technology (UOIT), Canada, as a faculty member, he was a postdoctoral fellow at Simon Fraser University (SFU), Canada. His research includes evolutionary algorithms, image processing, and opposition-based computation. Dr. Shahryar has been awarded the NSERC’s Japan Society for the Promotion of Science (JSPS) Fellowship, NSERC’s Industrial R&D Fellowship (IRDF), NSERC’s Visiting Fellowship in Canadian Government Laboratories (VF), the Canadian Institute of Health Research (CIHR) Fellowship for two times, and NSERC Discovery Grant.

**Zaid S. Mohamad** is M.Sc. student at the University of Ontario institute of Technology, he holds B.Sc. in Electrical Engineering since 1995. After graduation, he worked seven years as an Electronic Engineer in manufacturing sector, he moved to IT profession when he was hired by the United Nations as a network admin for their IT & telecommunication network in 2003. Since then, he has accumulated strong IT expertise in programming, networking, databases, and business intelligent. His current research is related to medical image segmentation and his research interests are computer vision, robotics, and image processing. In his spare time he likes to enjoy the nature with his wife and little daughter.